ORGANOMETALLICS
Communication
pubs.acs.org/Organometallics

Hydroxyl Radical Control through Hydrogen Bonding: Photolysis of Platinum(IV)hydroxido Complexes with Intramolecular H-Bonding

Lasantha A. Wickramasinghe and Paul R. Sharp*

125 Chemistry, University of Missouri, Columbia, Missouri 65211, United States

Supporting Information

ABSTRACT: By introducing hydrogen-bonding groups into the coordination sphere of Pt(IV) hydroxido complexes photogenerated hydroxyl radicals are tethered and directed to abstract a hydrogen atom from the ethyl group of a triethylphosphine ligand, even at 25 °C, to yield phosphaplatinacycle complexes.

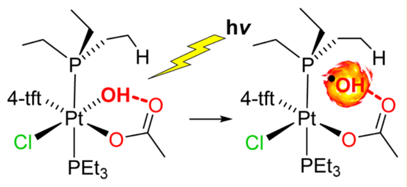

The hydroxyl (OH) radical is a notoriously promiscuous species reacting at near-diffusion-controlled rates with many compounds[1] and is important in atmospheric and combustion chemistry[2,3] and in biological systems.[4−6] It is believed to be involved in metal−oxygen chemistry including Fenton-type chemistry,[7,8] Shilov hydrocarbon oxidation,[9] and cytochrome P450 hydrocarbon hydroxylation.[10]

Recently, we discovered that photolysis of Pt(IV) hydroxido complexes generates OH radicals that can be constrained into intramolecular C−H abstraction from a PEt_3 ligand by photolyzing in a 77 K glassy matrix (Scheme 1, 4-tft = 4-trifluoromethylphenyl).[11] (Photolysis of organic compounds can also produce OH radicals.[12,13]) The constraints of the glassy matrix are thought to inhibit OH radical escape and/or its abstraction of an adjacent chlorido ligand, processes that occur at room temperature to give exclusively formal HOCl reductive-elimination product **3**.[14,15] Seeking to gain further control of the OH radical, we modified the complex by introducing ligands that form intramolecular hydrogen bonds to the hydroxido ligand. (Hydrogen bonding of the OH radical is believed to be important in enzyme systems.[4,10]) We now report reactivity for these new complexes that is similar to that of **1** in the 77 K matrix but in solution at room temperature.

Scheme 1

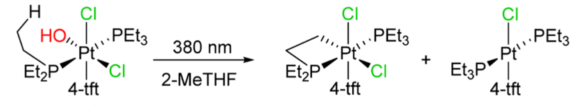

T °C	Yield of **2**
25 or -78	0%
-196	66%

The potential importance of intramolecular hydrogen bonding in the photochemistry of Pt(IV) hydroxido complexes was recently highlighted for *trans*-$Pt(PEt_3)_2(Cl)(OH)(OOH)$-(4-tft) (**4**) (tft = trifluoromethylphenyl), where DFT calculations suggested that the hydrogen-bonding pattern of the hydroxido and hydroperoxido ligands could affect the outcome of the photochemistry.[16] This inspired us to synthesize new Pt(IV) hydroxido complexes with carboxylate ligands (**5**, **6**, and **7**) in place of the hydroperoxo ligand by simple protonation of the OOH ligand in **4** with acids (Scheme 2). (A sulfate-bridged dimer, [*trans*-$Pt(PEt_3)_2Cl$(4-tft)-$(OH)]_2SO_4$, and a boric acid product that incorporates the OOH ligand, *trans*-$Pt(PEt_3)_2Cl$(4-tft)(OB(OH)OO), were also prepared by this method and characterized by X-ray crystallography.[17])

Scheme 2

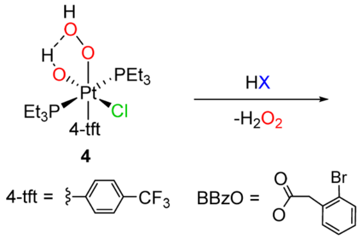

X = OAc (**5**)
CF_3CO_2 (**6**)
BBzO (**7**)
CN (**8**)

As shown by the solid-state structures for **5** (Figure 1) and **6**,[17] there is strong intramolecular hydrogen bonding between the carboxylato and the hydroxido ligands.[18] Complex **6** shows a slightly longer hydrogen bond to the carbonyl group than in **5** (O1--O3 = 2.840(6) Å for **6**, 2.815(3) Å for **5**), consistent with the expected weaker hydrogen bond acceptor properties of the trifluoroacetato ligand. The hydroxido ligand ^1H NMR resonances in **5**, **6**, and **7** also indicate hydrogen bonding and are downfield shifted compared to the hydroxido signal in non-hydrogen-bonded **1**.

Remarkably, photolysis (380 nm) of **5**−**7** at room temperature in CD_2Cl_2 gives C−H activation products phosphaplatinacycles **9**−**11** in yields as high as 50% (Scheme 3, Table 1). At −78 °C the yields of the phosphaplatinacycles increase to as high as 90%. The solvent choice for the photolysis is critical,

Received: April 7, 2015
Published: July 2, 2015

DOI: 10.1021/acs.organomet.5b00292
Organometallics 2015, 34, 3451−3454

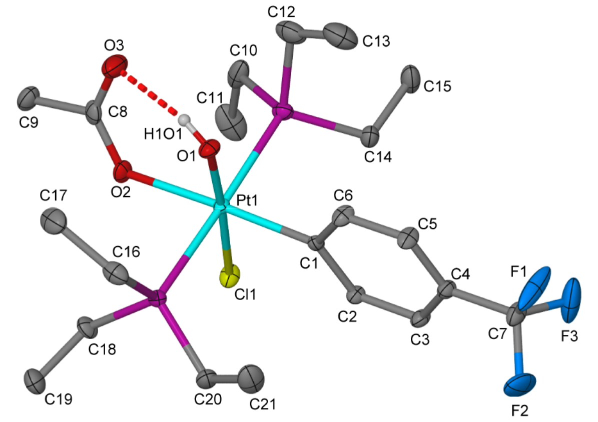

Figure 1. Drawing of the solid-state structure of *trans*-Pt$(PEt_3)_2$(4-tft)(Cl)(OH)(OAc), **5** (50% probability ellipsoids, C-bonded hydrogen atoms omitted). Rotational disorder in the CF_3 group is not shown. Distances (Å): O3−O1 = 2.815(3), O1−H1O1 = 0.75(3), O3--H1O1 = 2.11(3).

Scheme 3

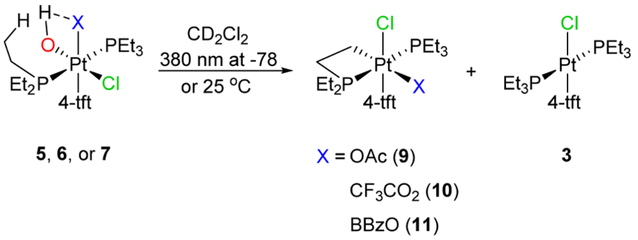

Table 1. Photolysis Products (%)[a] **from *trans*-Pt$(PEt_3)_2$(Cl)(X)(OH)(4-tft) in CD_2Cl_2**

X	−78 °C		25 °C	
	platinacycle	Pt(II)[b]	platinacycle	Pt(II)[b]
OAc (**5**)	90	10	50	50
O_2CCF_3 (**6**)	90	10	15	85
BBzO (**7**)	81	19	50	50
CN (**8**)	30	70	0	95[e]
Cl (**1**)	15[c]	45[c]	0	100
OAc (**5**) (in C_7H_8)	50[d]	50[d]	0	100

[a] Yields determined by ^{31}P NMR spectral integration. [b] Pt(II) = *trans*-Pt$(PEt_3)_2$(4-tft)X or *trans*-Pt$(PEt_3)_2$(4-tft)Cl. [c] $OPEt_3$ (24%) and other unidentified products also observed. [d] Same at 77 K (LN_2). [e] Remaining unidentified product observed at δ 17 (s) in the ^{31}P NMR spectrum.

and in toluene the yield of **9** from **5** is 0% at 25 °C and 50% at −78 °C. Since our original studies of **1** were in 2-MeTHF and toluene, we repeated the photolysis of **1** in CD_2Cl_2. As before, at 25 °C phosphaplatinacycle **2** is not detected and **3** is the only product. At −78 °C, some **2** is formed (15%), but the major products are **3** (45%) and $OPEt_3$ (24%).

Unfortunately, the phosphaplatinacycles are unstable to isolation[17] and were characterized in solution. The ^{31}P and ^{1}H NMR spectra[17] (for **9**) of **9**−**11** are similar to those for previously reported **2**.[11] Most diagnostic is the ^{31}P NMR high-field shift of the P atom in the four-membered ring. Strong coupling between this P atom and that of the PEt_3 ligand establishes a *trans* relationship. Signals for the platinum-bonded phosphaplatinacycle carbon atoms (C1) are also evident in the ^{13}C-DEPT NMR and HMQC NMR spectra[17] and show platinum coupling and two-bonded diastereotopic protons. What has changed with the new complexes is the ^{1}H NMR signals for the 4-tft ligand *ortho*-protons. Only one signal is observed for **2**, whereas **9** has two signals due to slow 4-tft rotation on the NMR time scale. As this change is most likely due to a change in the ligand *cis* to the 4-tft ligand, we assign the structures of **9**−**11** as shown in Scheme 3.

Monitoring the photolysis of **5** shows the formation of a second phosphaplatinacycle, **9′**. Both **9** and **9′** initially grow in together in a 1:1 ratio, but as the photolysis continues, **9′** converts to **9** (Scheme 4). We assign the structure of **9′** to the isomer of **9** where the chlorido ligand, instead of the OAc ligand, is *cis* to the 4-tft ligand (Scheme 4). Consistent with this assignment, the ^{1}H NMR spectrum of **9′** shows only one *ortho*-tft proton signal, the same as **2**, which also has a chlorido ligand *cis* to the 4-tft ligand. Careful examination of the ^{31}P NMR spectra[17] of **11** also reveals low concentrations of a second phosphaplatinacycle, which we assign as the isomer (**11′**) with the chlorido ligand *cis* to the 4-tft ligand, the same as **9′**. No other isomer is detected for **10**.

Scheme 4

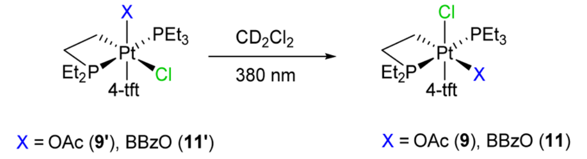

The above results suggest that intramolecular hydrogen bonding to the hydroxido group is an important factor in the formation of the phosphaplatinacycles. However, the *cis* ligand, which is subject to abstraction, has also been changed, and this may have suppressed the competitive formal reductive elimination to give **3**. We investigated this possibility by DFT (gas phase) and by the synthesis and photolysis of two other complexes. The DFT-calculated free energy of AcOOH reductive elimination for **5** was compared to the previously calculated value for HOCl reductive elimination from **1**. The values are essentially identical at 32.8 (**5**) and 32.3 kcal/mol (**1**), indicating that the net thermodynamics of the elimination are unchanged. The Cl radical and OAc radical removal energies from the Pt(III) doublets resulting from OH dissociation from **1** and **5** were also evaluated. Acetate radical removal from *trans*-Pt$(PEt_3)_2$(Cl)(OAc)(4-tft) takes only 17.3 kcal/mol, while Cl radical loss from *trans*-Pt$(PEt_3)_2Cl_2$(4-tft) requires 33.3 kcal/mol.[19] Clearly, replacement of the chlorido ligand in **1** with the acetato ligand in **5** does not appear likely to inhibit reductive elimination and explain the enhanced yield of phosphaplatinacycles for carboxylate complexes **5**−**7**.

In an attempt to experimentally suppress elimination, **8** was prepared with a cyanido ligand (Scheme 5). Despite the strongly bonded cyanido ligand *cis* to the OH ligand, photolysis

Scheme 5

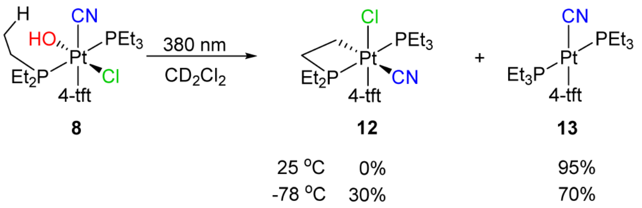

DOI: 10.1021/acs.organomet.5b00292
Organometallics 2015, 34, 3451−3454

of **8** at 25 °C yields only reductive elimination product *trans*-Pt$(PEt_3)_2$(CN)(4-tft) (Scheme 5) and no phosphaplatinacycle. Thus, with a strongly bonded *cis* ligand, and in the absence of hydrogen bonding, an alternate *trans* elimination occurs. However, at −78 °C a 30% yield of phosphaplatinacycle **12** is obtained. While not as high a phosphaplatinacycle yield as the hydrogen-bonded carboxylic acid systems, it is double the yield from **1**, suggesting that strong bonding of the *cis* ligand does slow reductive elimination and allow greater C−H activation.

Scheme 6

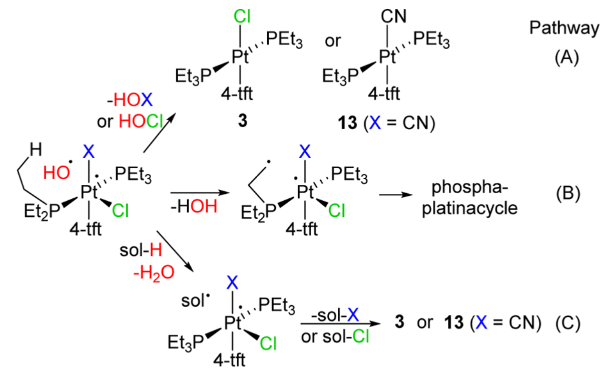

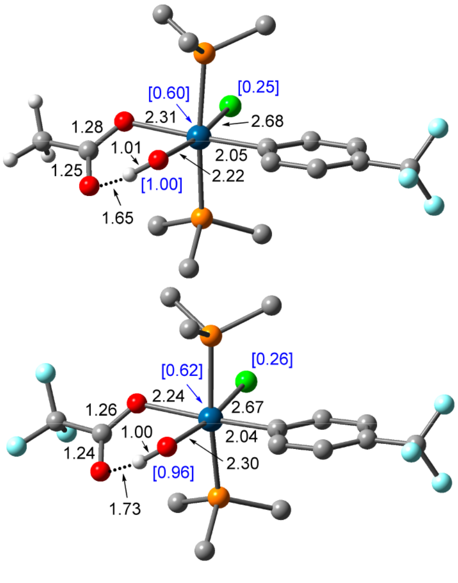

Figure 2. Drawings of the DFT triplets *trans*-Pt$(PEt_3)_2$(4-tft)(Cl)(OH)(OAc) (^{T}**5**, top) and *trans*-Pt$(PEt_3)_2$(4-tft)(Cl)(OH)(O_2CCF_3) (^{T}**6**, bottom) (hydrogen atoms omitted except for OH and OAc). Distances (Å) in black and Mulliken electron spin densities on Cl, Pt, and the OH in blue and brackets. Pt = blue, P = orange, Cl = green, F = light blue, O = red, C = gray.

The above results can be interpreted with the three photolysis pathways presented in Scheme 6. All three pathways start from the lowest energy triplet excited state, which has been previously modeled[11,14] with DFT for **1** and now for **5** and **6**. The model complexes (see below and Figure 2) show elongation of the Pt−OH bond and near-unity spin density on the OH group, indicating a weakly interacting Pt(III)/OH geminate radical pair. In pathway B a phosphine hydrogen atom abstraction by the OH radical gives water and, after ring closing, the phoshaplatinacycle. Competitive with this pathway are the net reductive elimination pathways A and C. In pathway A the OH radical abstracts a ligand from the Pt(III) center, while in pathway C a solvent hydrogen atom is first abstracted by the OH radical and then the resulting solvent radical abstracts a ligand from the Pt(III) center. Pathway C is favored with toluene and other solvents that contain relatively weakly bonded hydrogen atoms and when the OH radical escapes the coordination sphere of the Pt center. Pathway A generally results in abstraction of a *cis* ligand (*cis* elimination in closely related systems has been observed[14,16,19]), but in the case of **8**, where the CN ligand is strongly bonded, the OH radical can migrate and abstract the *trans* Cl ligand. Pathway B then is favored by OH radical tethering to the complex, preventing escape, migration, and ligand abstraction. Consistent with entropically unfavorable tethering, pathway B is more sensitive to temperature than pathways A and C, and the amount of pathway B product (phosphaplatinacycle) decreases from −78 °C to 25 °C. Indeed, the strength of the hydrogen-bond tethering is reflected in the yields. At −78 °C all three carboxylate complexes give comparable yields of phosphaplatinacycle that drop as the temperature is raised and the other pathways began to operate. However, the strongest hydrogen bonding is expected to be present in **5** and **7**, and these give 50% at 25 °C. Weaker hydrogen bonding in **6** limits the yield to 15% at 25 °C, where OH radical escape, migration, and/or ligand abstraction dominate.

The lowest energy triplet states (^{T}**5** for **5** and ^{T}**6** for **6**) were modeled by DFT to examine the hydrogen bonding and the spin density distribution. The optimized structures are given in Figure 2 and generally resemble the triplet previous found for **1**.[11,14] Both ^{T}**5** and ^{T}**6** show intramolecular hydrogen bonding between the carboxylate and hydroxido groups with distances that are shorter than in the singlet[17] model complexes. (Stronger hydrogen bonding is attributed to a more polar O−H bond in the radical.[20]) The OAc complex ^{T}**5** appears to have a particularly strong interaction with a remarkably short H--O distance of 1.65 Å (1.92 Å in the singlet[17]), consistent with strong tethering of the OH radical. The expected weaker hydrogen bond acceptor ability of the CF_3OAc ligand is evident in the longer O--H distance of 1.73 Å (1.97 Å in the singlet[17]), indicating a weaker tethering and more facile migration or escape of the OH radical. Spin density values (Figure 2) show the expected near-unity spin density on the OH moiety, indicating high radical character. Finally, escape of the OH radical from ^{T}**5** requires 8.7 kcal/mol, most of which would involve breaking the hydrogen bonding.

Finally, we sought to incorporate alternative hydroxido hydrogen bonding to enhance pathway B to the phosphaplatinacycle and replaced the 4-tft ligand with a 2-methoxyphenyl group to give **14**[17] (Scheme 7). Photolysis of **14** at −78 °C gives a 40% yield of phosphaplatinacycle **15**, improved from the 30% yield for analogous 4-tft complex **8**. This is not to the 90% level observed for **6**, but the hydrogen bonding of the

Scheme 7

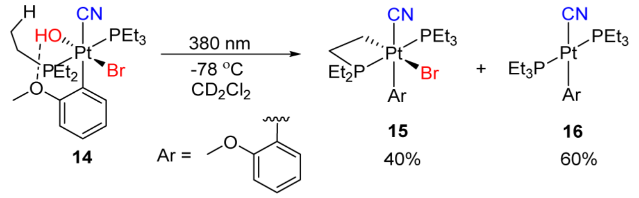

methoxyphenyl ligand to the hydroxido ligand should be relatively weak compared to that in the carboxylato complexes and the effect of changing the aryl group on the other pathways is unknown and could be significant.

In conclusion, we have shown that by incorporating hydrogen bonding into hydroxido complexes that are photoactive for OH radical generation we can tether the OH radical and direct its reactivity toward one pathway out of several, thus harnessing the radical to do selective chemistry. (Hydrogen-bonded hydroxyl radicals are thought to be involved in the mechanism of monooxygenases.[4])

■ ASSOCIATED CONTENT

Ⓢ Supporting Information

Experimental details, decomposition data for **9** and **9′**, NMR spectra, structural drawings, DFT energies and coordinates, X-ray structural details (cif). The Supporting Information is available free of charge on the ACS Publications website at DOI: 10.1021/acs.organomet.5b00292.

■ AUTHOR INFORMATION

Corresponding Author

*E-mail: sharpp@missouri.edu.

Author Contributions

All authors have given approval to the final version of the manuscript and contributed equally.

Notes

The authors declare no competing financial interest.

■ ACKNOWLEDGMENTS

Support was provided by the U.S. Department of Energy, Office of Basic Energy Sciences (DE-FG02-88ER13880). We thank Dr. Charles Barnes for X-ray data collection and processing and Dr. Wei Wycoff for assistance with the NMR measurements.

■ REFERENCES

(1) Mitroka, S.; Zimmeck, S.; Troya, D.; Tanko, J. M. *J. Am. Chem. Soc.* **2010**, *132*, 2907−2913,.

(2) Allodi, M. A.; Kirschner, K. N.; Shields, G. C. *J. Phys. Chem. A* **2008**, *112*, 7064−7071,.

(3) Carr, S. A.; Still, T. J.; Blitz, M. A.; Eskola, A. J.; Pilling, M. J.; Seakins, P. W.; Shannon, R. J.; Wang, B.; Robertson, S. H. *J. Phys. Chem. A* **2013**, *117*, 11142−11154,.

(4) Badieyan, S.; Bach, R. D.; Sobrado, P. *J. Org. Chem.* **2015**, *80*, 2139−2147,.

(5) Burrows, C. J.; Muller, J. G. *Chem. Rev.* **1998**, *98*, 1109−1152,.

(6) Pogozelski, W. K.; Tullius, T. D. *Chem. Rev.* **1998**, *98*, 1089−1108,.

(7) Fenton, H. J. H. *J. Chem. Soc., Trans.* **1894**, *65*, 899−910,.

(8) Bataineh, H.; Pestovsky, O.; Bakac, A. *Chem. Sci.* **2012**, *3*, 1594−1599,.

(9) Rudakov, E. S.; Shul'pin, G. B. *J. Organomet. Chem.* **2015**, DOI: 10.1016/j.jorganchem.2015.01.032.

(10) Bach, R. D.; Dmitrenko, O. *J. Am. Chem. Soc.* **2006**, *128*, 1474−1488,.

(11) Wickramasinghe, L. A.; Sharp, P. R. *Inorg. Chem.* **2014**, *53*, 11812−11814,.

(12) Boivin, J.; Crépon, E.; Zard, S. Z. *Tetrahedron Lett.* **1990**, *31*, 6869−6872,.

(13) Zhou, C.-H.; Cheng, S.-B.; Yin, H.-M.; He, G.-Z. *J. Phys. Chem. A* **2011**, *115*, 5062−5068,.

(14) For efforts to detect photogenerated HOCl see: Wickramasinghe, L. A.; Sharp, P. R. *Inorg. Chem.* **2014**, *53*, 1430−1442,.

(15) Net HOCl photoreductive elimination has been observed in the gas phase for $AuCl_2(OH)_2^-$: Marcum, J. C.; Kaufman, S. H.; Weber, J. M. *J. Phys. Chem. A* **2011**, *115*, 3006−3015,.

(16) Wickramasinghe, L. A.; Sharp, P. R. *J. Am. Chem. Soc.* **2014**, *136*, 13979−13982,.

(17) See Supporting Information.

(18) A similar intramolecular hydrogen-bonding pattern is observed in a platinum(IV) hydroxido phthalato complex: Pellarin, K. R.; McCready, M. S.; Sutherland, T. I.; Puddephatt, R. J. *Organometallics* **2012**, *31*, 8291−8300,.

(19) Perera, T. A.; Masjedi, M.; Sharp, P. R. *Inorg. Chem.* **2014**, *53*, 7608−7621,.

(20) Johnson, E. R.; Dilabio, G. A. *Interdiscip. Sci.: Comput. Life Sci.* **2009**, *1*, 133−140,.